

A \mathcal{PT} -symmetric dual-core system with the sine-Gordon nonlinearity and derivative coupling

J. Cuevas–Maraver

*Grupo de Física No Lineal, Departamento de Física Aplicada I,
Universidad de Sevilla. Escuela Politécnica Superior, C/ Virgen de África, 7, 41011-Sevilla, Spain
Instituto de Matemáticas de la Universidad de Sevilla (IMUS). Edificio Celestino Mutis. Avda. Reina Mercedes s/n, 41012-Sevilla, Spain*

B.A. Malomed

*Department of Physical Electronics, School of Electrical Engineering,
Faculty of Engineering, Tel Aviv University, Tel Aviv 69978, Israel*

P.G. Kevrekidis

Department of Mathematics and Statistics, University of Massachusetts, Amherst, MA 01003-4515, USA

We propose a system of sine-Gordon equations, with the \mathcal{PT} symmetry represented by balanced gain and loss in them. The equations are coupled by sine-field terms and first-order derivatives. The sinusoidal coupling stems from local interaction between adjacent particles in the coupled Frenkel-Kontorova (FK) chains and related sine-lattices, while the cross-derivative coupling, which was not considered before, is induced by *three-particle* interactions, provided that the particles in the parallel FK chains move in different directions. Nonlinear wave structures are then studied in this model. In particular, kink-kink (KK) and kink-antikink (KA) complexes are explored by means of analytical and numerical methods. It is predicted analytically and confirmed numerically that the complexes are unstable for one sign of the sinusoidal coupling, and stable for another. Stability regions are delineated in the underlying parameter space. Unstable complexes split into free kinks/antikinks that may propagate or become stationary, depending on whether they are subject to gain or loss, respectively.

I. INTRODUCTION

Dual-core waveguides with intrinsic nonlinearity carried by each core offer a convenient setting for the creation of stable dissipative solitons, by application of linear gain to one core, and leaving the parallel-coupled mate one lossy. This possibility was first proposed in the context of nonlinear optics in Ref. [1], see also a review in Ref. [2]. More recently, a similar scheme was elaborated for the application of gain and stabilization of solitons in plasmonics [3], as well as for the creation of stable two-dimensional dissipative solitons and solitary vortices in dual laser cavities [4]. Commonly adopted models of dual-core nonlinear waveguides are based on linearly coupled systems of nonlinear Schrödinger (NLS) equations, which include gain and loss terms [2, 5]. One of the advantages provided by these systems for the theoretical analysis is the availability of exact analytical solutions for stable solitons [6].

A crucial difference between dissipative solitons and their counterparts in conservative media is the fact that the former ones exist as isolated attractors, selected by the balance between gain and loss [7]. On the contrary, nonlinear conservative models, including those originating from optics [8], give rise to continuous families of soliton solutions, rather than isolated ones.

A more special class of systems was identified at the interface between conservative and dissipative ones, with spatially separated and precisely balanced loss and gain. Such systems realize the \mathcal{PT} (parity-time) symmetry, which originates in the quantum theory for non-Hermitian Hamiltonians [9]. A distinctive feature of the \mathcal{PT} -symmetric Hamiltonians is that they produce purely real spectra up to a certain critical value of the strength of the part which represents the balanced gain and loss. At the critical point, the \mathcal{PT} symmetry suffers breaking, with the Hamiltonian's spectrum becoming complex above this point.

Experimental implementation of the \mathcal{PT} symmetry was suggested by the fact that the classical propagation equation for optical beams in the paraxial approximation has essentially the same form as the quantum-mechanical Schrödinger equation, making it possible to emulate the evolution of the wave function of a quantum particle by the transmission of an optical beam [10]. Accordingly, the implementation of the \mathcal{PT} symmetry in optics was proposed in Ref. [11] and experimentally demonstrated in Ref. [12] (see also the early review [13] and the more recent one of [14]), making use of mutually balanced symmetrically placed gain and loss elements.

The presence of the Kerr effect in optical media suggests to consider the interplay of the \mathcal{PT} -symmetry with cubic nonlinearity, leading to the prediction of \mathcal{PT} -symmetric solitons [15]. A crucially important issue in theoretical studies of such solitons is the analysis of their stability, as the exact balance between the amplification and dissipation may be easily disrupted [16]. It was also proposed to implement a similar setting in atomic Bose-Einstein condensates, with the linear gain provided by a matter-wave laser [17]. Another possibility is to create the \mathcal{PT} symmetry in exciton-polariton condensates, which constitute genuinely open systems where the gain or pump is a necessary ingredient of any setting [18].

The above-mentioned couplers, with the gain and loss carried by different parallel-coupled cores, offer a natural platform for the realization of the \mathcal{PT} symmetry, if one takes care to exactly balance the gain and loss in the two cores [19, 20]. Adding the intrinsic Kerr nonlinearity, the analysis makes it possible to find \mathcal{PT} -symmetric solitons in the coupler and their stability

boundary in an exact analytical form [19]. In addition to the fundamental two-component solitons, higher-order ones [21] and soliton chains [22] in the \mathcal{PT} -symmetric coupler were also considered. Bilayer systems of other types with balanced gain and loss were investigated too [23].

An interesting extension of the analysis is to combine the linear \mathcal{PT} symmetry with other physically relevant nonlinearities, such as quadratic (alias second-harmonic-generating) [24] and sine-Gordon (SG) [25] ones. In particular, the SG nonlinearity finds its realizations in a broad range of physical settings [26], including various forms of the Frenkel-Kontorova (FK) model [27, 28], long Josephson junctions (JJs) between bulk superconductors [29], self-induced transparency [30], ferromagnets [31], ferroelectrics [32], and field-theory models [33]. In all these realizations, fundamental dynamical modes are topological solitons (kinks and antikinks) [34]. In particular, they represent fluxons and antifluxons, i.e., magnetic-flux quanta trapped in long JJs [29].

A natural possibility is to implement the \mathcal{PT} symmetry in couplers, composed of an amplified core and a dissipative one, as outlined above, in the case when each core hosts the SG dynamics. Previously, many works have addressed models based on coupled SG equations [34, 35], such as those modeling double FK chains [27], stacked JJs [36–38] and the layered structure of high-temperature superconductors [39]. However, the competition of the gain and loss acting in the two coupled SG cores was not considered before. This is the subject of the present work. The basic \mathcal{PT} -symmetric coupled-SG model is formulated in Sec. II, where conditions for the background stability of the system are derived too. The dual system is supported by two couplings, one presented by previously known sinusoidal terms [27, 38], and a previously unexplored coupling, based on the first-order cross-derivatives, which represent a *three-body* interaction between adjacent particles in an underlying double FK chain, with different directions of motion of the particles in the two individual chains. Fundamental topological modes in the system are built as kink-kink (KK) and kink-antikink (KA) complexes (in addition to them, nontopological small-amplitude breathers are briefly considered too). Analytical and numerical results for the KK and KA states are reported in Secs. III and IV. The most essential results are existence and stability boundaries for the KK and KA states, delineated in the underlying parameter space by means of analytical and numerical methods. The paper is concluded by Sec. V, suggesting also some potential extensions to future work.

II. THE MODEL

A. The coupled sine-Gordon system

The \mathcal{PT} -symmetric system of coupled SG equations for two real fields, amplified field $\phi(x, t)$ and attenuated field $\psi(x, t)$, is adopted in the following form:

$$\phi_{tt} - \phi_{xx} + \sin \phi = \epsilon \sin(\phi - \psi) + \beta \psi_x + \alpha \phi_t, \quad (1)$$

$$\psi_{tt} - \psi_{xx} + \sin \psi = \epsilon \sin(\psi - \phi) - \beta \phi_x - \alpha \psi_t, \quad (2)$$

where α is the coefficient accounting for the balanced gain and loss, and ϵ is the coefficient of the inter-chain sinusoidal coupling in the double FK chain [27] (a similar coupling appears in a triangular system of three long JJs with a trapped magnetic flux [38]). Such sinusoidal coupling has also been considered extensively in the setting of the so-called sine-lattices [40], used e.g. in base rotator models of the double helix of DNA [41]. The coefficient β represents a new type of the anti-symmetric cross-derivative coupling between the two SG equations (note that reflection $x \rightarrow -x$ makes it possible to choose the sign of β arbitrarily). It is different from the usual magnetic coupling between stacked JJs, which would be represented by symmetric second-order cross-derivatives [36]. The Hamiltonian corresponding to the conservative version of Eqs. (1) and (2), with $\alpha = 0$, is

$$H = \int_{-\infty}^{+\infty} \left[\frac{1}{2} (\phi_t^2 + \psi_t^2 + \phi_x^2 + \psi_x^2) + (1 - \cos \phi) + (1 - \cos \psi) - \epsilon (1 - \cos(\phi - \psi)) - \beta \phi \psi_x \right] dx. \quad (3)$$

The Hamiltonian of Eq. (3) can also be rewritten with the last term in the integrand replaced by its symmetrized form, $-(\beta/2)(\phi \psi_x - \psi \phi_x)$.

The anti-symmetric cross-derivative coupling emerges in a “triangular” dual FK system schematically displayed in Fig. 1. It is assumed that particles with coordinates $v_n(t)$ belonging to the bottom chain may move in the horizontal direction, while particles with coordinates $u_n(t)$, which belong to the top chain, move along a different direction, under fixed angle θ with respect to the horizontal axis. In this system, the usual local coupling between the top and bottom chains may be interpreted as produced by energies of diagonal springs linking adjacent particles. These energies are, in turn, determined by squared lengths of these links. In particular, the sum of the squared lengths for the pair of links connecting the n -th particle in the top chain to its neighbors,

with numbers n and $n + 1$, is

$$\begin{aligned} l_{n,n}^2 + l_{n,n+1}^2 &= 2(h + u_n \sin \theta)^2 + \left(\frac{a}{2} + u_n \cos \theta - v_n\right)^2 + \left(\frac{a}{2} - u_n \cos \theta + v_{n+1}\right)^2 \\ &\equiv \frac{a^2}{2} + 2h^2 + a(v_{n+1} - v_n) + 4h(\sin \theta)u_n + 2u_n^2 + v_n^2 + v_{n+1}^2 - 2(\cos \theta)u_n(v_n + v_{n+1}), \end{aligned} \quad (4)$$

where a and h are the spacing in each FK chain, and the separation between the parallel chains, respectively. A straightforward consideration of the continuum limit for the corresponding FK Hamiltonian, which corresponds to

$$\{u_n(t), v_n(t)\} \rightarrow \{\phi(x, t), \psi(x, t)\}, \quad an \rightarrow x, \quad (5)$$

demonstrates that the last term in expression (4) represents the local-coupling energy, which indeed gives rise to the linearized form $[\sin(\phi - \psi) \approx \phi - \psi]$ of terms $\sim \epsilon$ in Eqs. (1) and (2), so that $\cos \theta \sim -\epsilon$ (the most essential results are obtained below for $\epsilon < 0$, which corresponds to $\cos \theta \sim -\epsilon > 0$). Other terms in Eq. (4) do not represent the inter-chain coupling, and may be absorbed into an appropriate definition of the Hamiltonian of each chain. In particular, term $a(v_{n+1} - v_n)$ becomes a derivative $\sim \psi_x$ in the continuum limit, hence this term gives no contribution to the continuum Hamiltonian.

On the other hand, the cross-derivative couplings $\sim \beta$ may be induced by *three-particle* interactions (TPIs) in the underlying FK system, as usual binary interactions cannot give rise to this coupling (FK models with TPIs were considered in few previous works [42]). In the simplest case, the energy of the relevant TPI can be defined to be proportional to the sum of areas of the respective three-body triangles, as shown in Fig. 1. (i.e., the TPI is induced by the “surface tension” of the triangles). Interactions of this type may be realized in heterogeneous structures with FK chains attached to nanolayers which provide the surface tension, such as graphene (by dint of a technique similar to that reported in Ref. [43]) or other materials (see, e.g., Ref. [44]). This type of the TPI may also be adopted as a relatively simple phenomenological model.

To derive the cross-derivative-coupling term in the Hamiltonian induced by the TPI, we note that the area of the triangle, confined by the links whose lengths are given by Eq. (4), is

$$A_{n,n,n+1} = \frac{1}{2} [ah + h(v_{n+1} - v_n) + (\sin \theta)au_n + (\sin \theta)(v_{n+1} - v_n)u_n]. \quad (6)$$

It is easy to see that the transition to the continuum limit as per Eq. (5) transforms the last term in Eq. (6) into the last term in the Hamiltonian density corresponding to Eq. (3), with $\beta \sim -\sin \theta$, while the term $h(v_{n+1} - v_n)$ in expression (6), similar to its above-mentioned counterpart $a(v_{n+1} - v_n)$ in Eq. (4), becomes a derivative, ψ_x , in the continuum limit, hence it may be dropped from the Hamiltonian. Also, the term $(\sin \theta)au_n$ may be absorbed into the definition of the single-chain FK Hamiltonian. The onsite cosinusoidal terms in the Hamiltonian, viz., $\cos(2\pi u_n/b)$ and $\cos(2\pi v_n/b)$, may have $b \ll a$, if the FK chains are built as superlattices on top of an underlying lattice potential; then, kinks, which are considered below, will represent a relatively weak deformation of the chains.

Lastly, the above considerations demonstrate that the “polarization angle”, θ , in the dual-FK chain (see Fig. 1) determines the relative strength of the two couplings:

$$\beta/\epsilon \sim \tan \theta. \quad (7)$$

This relation shows that the cross-derivative coupling, $\beta \neq 0$, emerges when the motion directions in the coupled FK chains are not parallel ($\theta \neq 0$), while the usual coupling, with $\epsilon \neq 0$, acts unless the two directions are mutually perpendicular, $\theta \neq \pi/2$.

The \mathcal{PT} transformation for the system of Eqs. (1) and (2) is defined as follows:

$$\phi \equiv \tilde{\psi}, \psi = \tilde{\phi}, x = -\tilde{x}, t = -\tilde{t}. \quad (8)$$

It includes the swap of ψ and ϕ as the \mathcal{P} transformation in the direction transverse to x , as in usual \mathcal{PT} -symmetric couplers [19, 20]. Obviously, the system is invariant with respect to transformation (8).

B. Conditions for stability of the flat states

As the objective of the work is to produce KK and KA complexes, which interpolate between flat states with $\phi, \psi = 0 \pmod{2\pi}$, and explore stability of the complexes, a necessary preliminary condition is the stability of the flat states themselves against small perturbations. To address this issue, we use the linearized version of Eqs. (1) and (2), which governs the evolution of small perturbations around the flat states:

$$\phi_{tt} - \phi_{xx} + (1 - \epsilon)\phi + \epsilon\psi = \beta\psi_x + \alpha\phi_t, \quad (9)$$

$$\psi_{tt} - \psi_{xx} + (1 - \epsilon)\psi + \epsilon\phi = -\beta\phi_x - \alpha\psi_t. \quad (10)$$

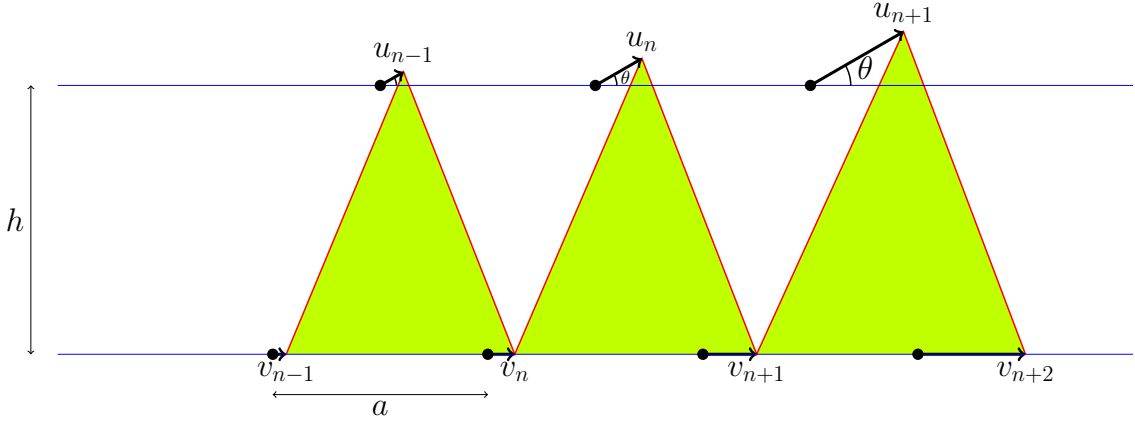


FIG. 1: (Color online) Three cells of the underlying double FK chain. Vectors show displacements of the particles in the top and bottom chains. The energy of the local two-particle coupling between the chains, which gives rise to terms $\sim \epsilon$ in Eqs. (1) and (2), is determined by squared lengths of the red links, see Eq. (4). The total energy of the three-particle coupling, which generates terms $\sim \beta$ Eqs. (1) and (2), is proportional to the combined area of the shaded triangles, see Eq. (6). The polarization angle θ of the motion in the top chain determines the relative strength of the two couplings in Eqs. (1) and (2) as per Eq. (7). Other details of the setting are explained in the text.

The substitution of the natural ansatz for eigenmodes of small perturbations, $\{\phi, \psi\} = \{\phi_0, \psi_0\} \exp(ikx - i\omega t)$, in Eqs. (9) and (10) yields the biquadratic dispersion equation for the eigenfrequency ω :

$$(\omega^2)^2 - 2 \left(1 - \epsilon + k^2 - \frac{\alpha^2}{2} \right) \omega^2 + (1 - \epsilon + k^2)^2 - \epsilon^2 - \beta^2 k^2 = 0. \quad (11)$$

Straightforward algebraic manipulations demonstrate that Eq. (11) gives rise to a purely real, i.e., instability-free spectrum, with $\omega^2(k^2) \geq 0$ for all $k^2 \geq 0$, under the following conditions:

$$\epsilon \leq 1/2, \quad (12)$$

$$\beta^2 \leq 2 \left[(1 - \epsilon) + \sqrt{1 - 2\epsilon} \right], \quad (13)$$

$$\alpha^2 \leq \beta^2, \quad (14)$$

$$\alpha^2 \leq 2 \left[(1 - \epsilon) - \sqrt{1 - 2\epsilon} \right]. \quad (15)$$

Note that, if ϵ satisfies constraint (12), then the expression on the right-hand side of Eq. (15) is always non-negative, i.e., the corresponding stability interval for α^2 consists of a finite (non-vanishing) interval of relevant values.

C. The small-amplitude limit: coupled NLS equations

Small-amplitude solutions to Eqs. (1) and (2) for oscillatory nontopological solitons (breathers) may be looked for as

$$\phi(x, t) = 2e^{-i(1-\epsilon/2)t} U(x, t) + \text{c.c.}, \quad \psi(x, t) = 2e^{-i(1-\epsilon/2)t} V(x, t) + \text{c.c.}, \quad (16)$$

where U and V are small-amplitude slowly varying complex functions, and c.c. stands for the complex conjugate. In the lowest order nontrivial approximation, the complex amplitudes obey a system of coupled NLS equations, which is derived from Eqs. (1) and (2):

$$iU_t + \frac{1}{2}U_{xx} + |U|^2U = \frac{\epsilon}{2}V - \frac{1}{2}\beta V_x + \frac{1}{2}i\alpha U, \quad (17)$$

$$iV_t + \frac{1}{2}V_{xx} + |V|^2V = \frac{\epsilon}{2}U + \frac{1}{2}\beta U_x - \frac{1}{2}i\alpha V. \quad (18)$$

The dispersion relation for the linearized version of Eqs. (17) and (18) yields

$$\omega = \frac{1}{2} \left(k^2 \pm \sqrt{\epsilon^2 - \alpha^2 + \beta^2 k^2} \right), \quad (19)$$

cf. Eq. (11), hence the zero-background solution is stable under the condition of $\alpha^2 < \epsilon^2$, which is not affected by coefficient β , cf. Eqs. (12)-(15). Note that the expansion of Eq. (15) for small ϵ leads to the same condition, illustrating the consistency of the relevant considerations.

The system of coupled NLS equations (17) and (18) with $\beta = 0$ is identical to the above-mentioned model of the \mathcal{PT} -symmetric coupler, which may be realized in terms of nonlinear fiber optics, admitting an exact analytical solution for solitons and their stability [19]. The additional terms $\sim \beta$ in the coupler model are known in fiber optics as representing the temporal dispersion of the coupling strength [45] (in that case, t and x are replaced, respectively, by the propagation distance and reduced time [8]). Solitons and their stability in the framework of Eqs. (17) and (18) with $\beta \neq 0$ constitute a separate problem which will be considered elsewhere. Hereafter, we will instead focus our considerations of this first work on this system to complexes in the form of topological kink structures.

III. ANALYTICAL RESULTS FOR KINK-KINK (KK) AND KINK-ANTI-KINK (KA) COMPLEXES

A. Stationary equations

Quiescent solutions to Eqs. (1) and (2), $\phi(x)$ and $\psi(x)$, satisfy the stationary equations,

$$\frac{d^2\phi}{dx^2} = \sin\phi - \epsilon \sin(\phi - \psi) - \beta \frac{d\psi}{dx}, \quad (20)$$

$$\frac{d^2\psi}{dx^2} = \sin\psi - \epsilon \sin(\psi - \phi) + \beta \frac{d\phi}{dx}, \quad (21)$$

which may be considered (with x replaced by time) as equations of two-dimensional motion of a mechanical particle of unit mass in the plane with coordinates (ϕ, ψ) , under the action of the Lorentz force $\sim \beta$ and a force produced by an effective potential, $U(\phi, \psi) = -(1 - \cos\phi) - (1 - \cos\psi) + \epsilon[1 - \cos(\phi - \psi)]$, cf. expression (3) for the Hamiltonian of the full SG system. As indicated above, we are interested in solutions for KK and KA complexes interpolating between different flat states, i.e., fixed points (FPs) of Eqs. (20) and (21), ϕ_0 and ψ_0 . The FPs are determined by equations

$$\begin{aligned} \sin\phi_0 &= -\sin\psi_0, \\ \epsilon \sin(\phi_0 - \psi_0) &= \sin\phi_0. \end{aligned} \quad (22)$$

It is easy to see that Eq. (22) gives rise to three sets of the FPs,

$$\phi_0 = \psi_0 = 2\pi n, \quad (23)$$

$$\phi_0 = \psi_0 = \pi(1 + 2n), \quad (24)$$

$$\phi_0 = 2\pi n, \psi_0 = \pi(1 + 2n), \quad (25)$$

with arbitrary integer n . Formally, also possible are FPs with $(\phi_0, \psi_0) = \pm \arccos(1/2\epsilon) + 2\pi n$ at $|\epsilon| > 1/2$; however, we do not consider them further due to the requirement (12) for the stability of the trivial solution.

It is easy to see that the Hamiltonian density defined by Eq. (3) has a minimum only at FP (23), while FPs (24) and (25) correspond to a maximum or saddle point, respectively, hence stable FPs may be produced solely by Eq. (23) [for this reason, the detailed stability analysis, which produces conditions (12)-(15), was presented above only for this type of the FP]. The KK and KA complexes should connect the FPs with different values of n , hence these complexes represent heteroclinic trajectories of the dynamical system based on Eqs. (20) and (21).

Note that the gain-loss coefficient, α , does not appear in Eqs. (20) and (21), hence it has no bearing on the shape of stationary states. Nevertheless, α does affect stability of KK and KA complexes, as shown below. This is similar to what has also been shown earlier in \mathcal{PT} -symmetric SG models in [25].

B. Exact solutions for $\beta = 0$

In the case of $\beta = 0$, stationary equations (20) and (21) admit two obvious types of solutions. One of them is symmetric,

$$\phi_0(x) = \psi_0(x), \quad (26)$$

with $\phi_0(x)$ being any stationary solution of the usual sine-Gordon equation,

$$\frac{d^2\phi_0}{dx^2} = \sin\phi_0, \quad (27)$$

such as the 2π kink, antikink, or periodic kink chains.

In the absence of the gain and loss terms, $\alpha = 0$, the stability of the symmetric solutions, with $\beta = 0$ can be investigated in the general form. Indeed, eigenmodes of small perturbations added to solution (26) can be looked for as symmetric or antisymmetric ones:

$$\{\phi(x, t), \psi(x, t)\} = \{\phi_0(x), \phi_0(x)\} + \zeta e^{-i\omega_\epsilon t} \phi_1^{(\pm)}(x) \{1, \pm 1\}, \quad (28)$$

where ζ is an infinitesimal amplitude of the perturbation, ω_ϵ is an eigenfrequency of the perturbation mode, and $\phi_1^{(\pm)}(x)$ are the eigenmodes themselves. The stability condition is that all eigenfrequencies must be real, $\omega_\epsilon^2 \geq 0$.

The linearization of the nonstationary coupled SG equations (1) and (2) (with $\beta = \alpha = 0$) leads to the following equations for the modal functions, $\phi_1^{(\pm)}(x)$:

$$\omega_\epsilon^2 \phi_1^{(+)} = -\frac{d^2 \phi_1^{(+)}}{dx^2} + [\cos \phi_0(x)] \phi_1^{(+)}, \quad (29)$$

$$(\omega_\epsilon^2 + 2\epsilon) \phi_1^{(-)} = -\frac{d^2 \phi_1^{(-)}}{dx^2} + [\cos \phi_0(x)] \phi_1^{(-)}. \quad (30)$$

Obviously, solutions of Eq. (29) have the same eigenvalues, $\omega_\epsilon^2 \equiv \omega_0^2$, as in the case of the usual single SG equation. In particular, the usual SG 2π kink (or antikink), see Eq. (41) below, is commonly known to be stable, hence it gives rise to $\omega_0^2 \geq 0$. Thus, the symmetric perturbations cannot destabilize the KK complex in the coupled system.

On the other hand, Eq. (30) for the antisymmetric perturbations gives rise to eigenvalues

$$\omega_\epsilon^2 = \omega_0^2 - 2\epsilon. \quad (31)$$

Note that Eq. (29) has a *zero-mode* solution, with $\omega_0 = 0$:

$$\phi_1^{(0)}(x) = \frac{d\phi_0}{dx}. \quad (32)$$

Then, the substitution of $\omega_0^2 = 0$ in Eq. (31) gives rise to $\omega_\epsilon^2 = -2\epsilon$. Thus, the symmetric KK solution of the coupled SG system is *unstable* for $\epsilon > 0$, and *stable* for $\epsilon < 0$.

The other type of solutions to stationary equations (20) and (21) with $\beta = 0$ is antisymmetric,

$$\phi_0(x) = -\psi_0(x), \quad (33)$$

with $\phi_0(x)$ being any solution of the stationary *double SG* equation,

$$\frac{d^2 \phi_0}{dx^2} = \sin \phi_0 - \epsilon \sin(2\phi_0). \quad (34)$$

An exact 2π -kink solution to Eq. (34), which corresponds to the antisymmetric KA complex produced by the coupled SG system, has the known form [46]:

$$\phi_0(x) = \pi + 2 \arctan \left(\frac{\sinh(\sqrt{1-2\epsilon}x)}{\sqrt{1-2\epsilon}} \right). \quad (35)$$

In the limit of $\epsilon = 0$, this solution is tantamount to the usual 2π kink. Obviously, solution (35) exists at $\epsilon < 1/2$, which agrees with condition (12). In the limit of $\epsilon = 1/2$, Eq. (35) takes a limit form, which is a relevant solution too, in this special case:

$$\phi_0^{(\epsilon=1/2)}(x) = \pi + 2 \arctan x. \quad (36)$$

At $\epsilon > 1/2$, a valid solution can be obtained from Eq. (35) by analytic continuation, in the form of a spatially periodic state (essentially, a KA chain):

$$\phi_0(x) = \pi + 2 \arctan \left(\frac{\sin(\sqrt{2\epsilon-1}x)}{\sqrt{2\epsilon-1}} \right). \quad (37)$$

All KA chains are unstable [26], hence solution (37) is unstable too.

The analysis of the stability of the KA complex, represented by solution (35) in the framework of coupled SG equations (1) and (2), is not analytically tractable, even in the case of $\beta = \alpha = 0$. The respective numerical results are presented below – see, in particular, Figs. 3, 7 and 8.

C. Perturbative solutions for small β

If the cross-derivative coupling constant β in Eqs. (20) and (21) is treated as a small perturbation, it is easy to see that the first correction to the symmetric KK solution (26), which was obtained above for $\beta = 0$, is antisymmetric. Thus, the full solution becomes asymmetric at $\beta \neq 0$:

$$\{\phi(x), \psi(x)\} = \{\phi_0(x) + \beta\phi_1(x), \phi_0(x) - \beta\phi_1(x)\}, \quad (38)$$

with $\phi_1(x)$ determined by the linearized equation

$$\frac{d^2\phi_1}{dx^2} - (\cos\phi_0(x))\phi_1 + 2\epsilon\phi_1 = -\frac{d\phi_0}{dx}. \quad (39)$$

It is easy to find an *exact solution* to Eq. (39), making use of the zero mode (32):

$$\phi_1(x) = -\frac{1}{2\epsilon} \frac{d\phi_0}{dx}. \quad (40)$$

In particular, the unperturbed 2π kink/antikink is

$$\phi_0(x) = 4 \arctan(e^{\sigma x}), \quad (41)$$

with polarity $\sigma = +1/-1$. The respective perturbed KK solution (38) is

$$\{\phi(x), \psi(x)\} = \left\{ 4 \arctan(e^{\sigma x}) - \frac{\beta\sigma}{\epsilon \cosh x}, 4 \arctan(e^{\sigma x}) + \frac{\beta\sigma}{\epsilon \cosh x} \right\}. \quad (42)$$

Below, these approximate analytical results are compared to their numerically found counterparts in Fig. 2.

Similarly, the first correction to the antisymmetric KA solution (33), induced by small β , must be symmetric, cf. Eq. (38), hence the corresponding full solution is again asymmetric:

$$\{\phi(x), \psi(x)\} = \{\phi_0(x) + \beta\phi_1(x), -\phi_0(x) + \beta\phi_1(x)\},$$

with ϕ_1 determined by the linearized equation (cf. Eq. (39))

$$\frac{d^2\phi_1}{dx^2} - (\cos\phi_0(x))\phi_1 = \frac{d\phi_0}{dx}. \quad (43)$$

However, it is not obvious how to identify a solution to Eq. (43) in an exact form, unlike solution (40) of Eq. (39). Below, stationary solutions for the KA complexes are found in a numerical form, see Fig. 2.

IV. NUMERICAL RESULTS FOR KINK-KINK (KK) AND KINK-ANTI-KINK (KA) COMPLEXES

A. Stationary KK and KA solutions and stability equations

In this section, we report results for KK and KA solutions of the full coupled system of SG equations (1) and (2) and their stability, obtained by means of numerical methods and complementing the analytical results of the previous section. Computations were performed with the help of a finite-difference scheme for the spatial derivatives, using a central-difference scheme for the first-order ones, and free-end (Neumann) boundary conditions.

Figure 2 shows profiles of solutions of both the KK and KA types at $\epsilon > 0$ and $\epsilon < 0$. For the KK complexes, we display the central part of the ϕ and ψ components, and compare them to the perturbative prediction given by Eq. (42); for the KA modes, we display both components only in the numerical form, as a fully analytical expression is not readily available for the perturbative solution of Eq. (43).

To study the spectral stability of the solutions, we proceed by adding small perturbations to the stationary solutions as follows:

$$\begin{aligned} \phi(x, t) &= \phi_0(x) + \delta u_1(x)e^{\lambda t}, \\ \psi(x, t) &= \psi_0(x) + \delta u_2(x)e^{\lambda t}, \\ \phi_t(x, t) &= \delta v_1(x)e^{\lambda t}, \\ \psi_t(x, t) &= \delta v_2(x)e^{\lambda t}, \end{aligned} \quad (44)$$

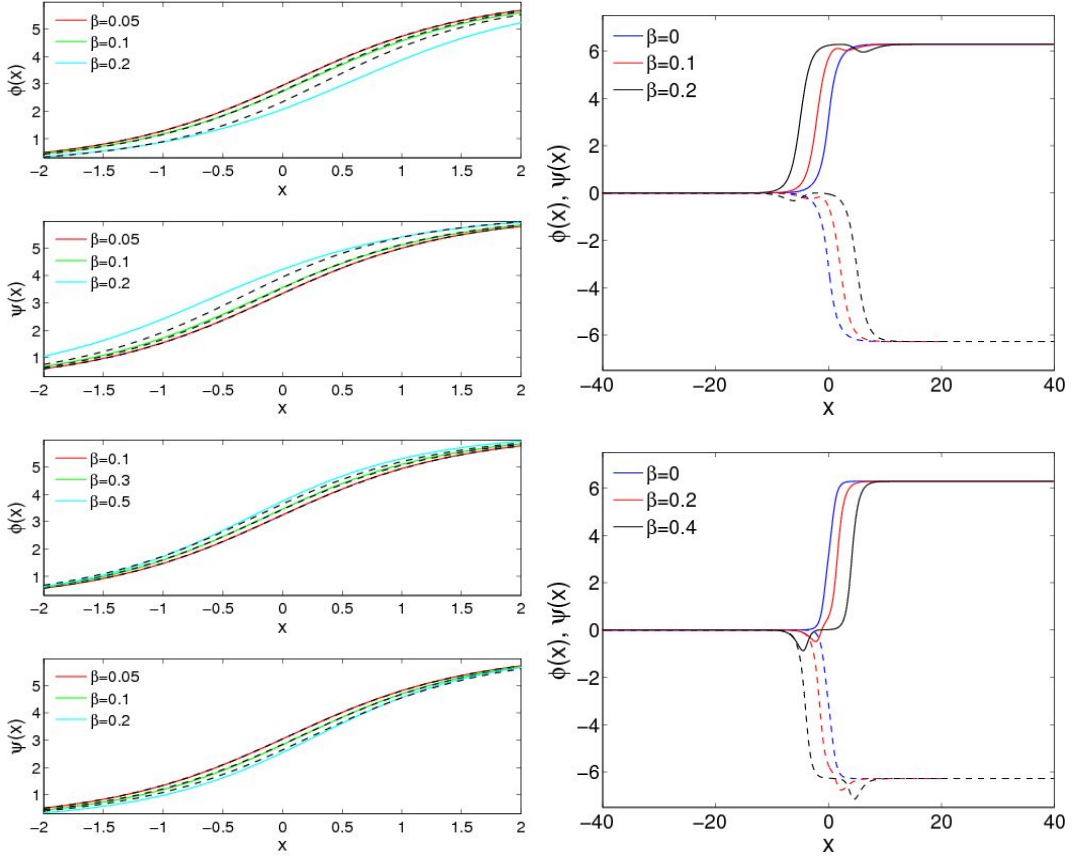


FIG. 2: (Color online) Profiles of the KK (left) and KA (right) complexes for $\epsilon = 0.25$ (top) and $\epsilon = -1$ (bottom), in both cases. In the former case, only the central parts of $\phi(x)$ and $\psi(x)$ are shown, and the profiles are compared to the approximate analytical solution given by Eq. (42), which is depicted by dashed lines. In the latter case, both $\phi(x)$ and $\psi(x)$ are shown in the same plot, respectively by full and dashed lines, respectively. The solutions are unstable at $\epsilon > 0$ (in the top panels) and stable at $\epsilon \leq 0$ (in the bottom panels).

where λ is a (generally, complex) (in)stability eigenvalue, $u_{1,2}(x)$ and $v_{1,2}(x)$ being the corresponding eigenmodes of the small perturbations. The spectral stability condition is that there should not exist eigenvalues with $\text{Re}(\lambda) > 0$. The substitution of expression (44) into Eqs. (1)-(2) and the subsequent linearization to $\mathcal{O}(\delta)$ leads to the following eigenvalue problem:

$$\lambda \begin{pmatrix} u_1 \\ u_2 \\ v_1 \\ v_2 \end{pmatrix} = \begin{pmatrix} 0 & 0 & I & 0 \\ 0 & 0 & 0 & I \\ \epsilon \cos(\phi_0 - \psi_0) - \cos(\phi_0) + \partial_{xx} & -\epsilon \cos(\phi_0 - \psi_0) + \beta \partial_x & \alpha I & 0 \\ -\epsilon \cos(\phi_0 - \psi_0) - \beta \partial_x & \epsilon \cos(\phi_0 - \psi_0) - \cos(\psi_0) + \partial_{xx} & 0 & -\alpha I \end{pmatrix} \begin{pmatrix} u_1 \\ u_2 \\ v_1 \\ v_2 \end{pmatrix}, \quad (45)$$

with I being the identity operator. As said above, the KK profiles do not depend on the gain-loss coefficient α , although their stability does depend on α , through its explicit inclusion inside the matrix of Eq. (45).

Instabilities are not only caused by the existence of localized KK or KA complexes, but can also emerge from the background if conditions (12)-(15) are not fulfilled. In particular, if only Eqs. (12) and/or (13) are violated, background eigenvalues with nonzero real parts possess a zero imaginary part. On the other hand, if solely Eqs. (14) and/or (15) are violated, the respective unstable background eigenvalues have nonzero imaginary parts, with a slight difference between the two cases: if condition (14) is violated, the eigenvalues with nonzero real parts are those which possess the largest imaginary part, whereas, if condition (15) fails, unstable eigenvalues arise with the smallest imaginary part (i.e., close to wavenumbers $k = 0$).

B. Instability of the KK and KA complexes at $\epsilon > 0$

Both KK and KA complexes are found to be exponentially unstable at $\epsilon > 0$, in agreement with the exact analytical result obtained above for the KK complexes in the case of $\beta = \alpha = 0$ [see Eq. (31)]. Further, the complexes of both types exist, at

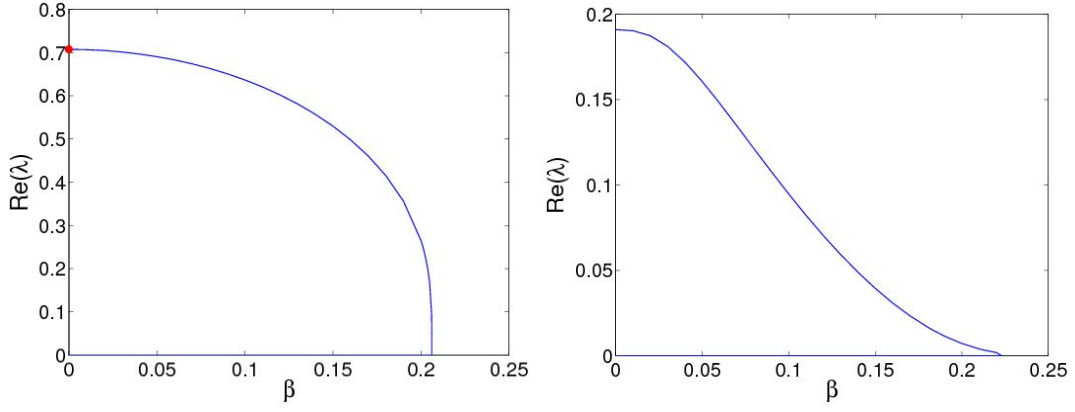


FIG. 3: (Color online) The real part of the instability eigenvalues versus β for unstable KK (left) and KA (right) complexes at $\alpha = 0$ and $\epsilon = 0.25$. They exist up to the point at which $\text{Re}(\lambda)$ vanishes. The red dot at the left panel shows the exact prediction for the zero mode of (31).

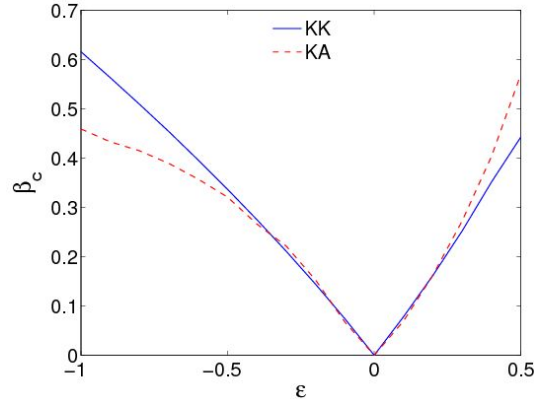


FIG. 4: (Color online) The critical value of the cross-derivative coupling, β_c , above which the KK and KA complexes do not exist, versus ϵ . Note that both complexes exist beyond the right edge (at $\epsilon \geq 0.5$); however, as condition (12) does not hold in that area, the flat states are unstable in it.

$\epsilon > 0$, below a critical point, $\beta < \beta_c$, which depends on ϵ . For given ϵ , the critical values β_c are different for the KK and KA solutions. At $\beta = \beta_c$, the real eigenvalue responsible for the kink's instability vanishes. Actually, β_c satisfies inequality (13), i.e., the existence range is smaller than the range of the background stability whenever Eqs. (14) and (15) hold. Figure 3 shows the dependence of the real part of the instability eigenvalues on β for fixed $\epsilon = 0.25$. Figure 4 shows the dependence of β_c on ϵ for both KK and KA complexes.

This instability leads to motion of the kinks, with the different components moving in opposite directions, i.e., the instability splits the KK and KA complexes, as shown in Figs. 5 and 6. Notice that, at $\alpha = 0$, the kinks move at constant velocities, with equal absolute values of the velocities in the two components, ϕ and ψ . However, at $\alpha \neq 0$, the kinks move with monotonously varying velocities, whose absolute values in the two components are different. In the latter case, the kink in the gain component accelerates, while that of the lossy component—in a way reminiscent to observations in [25]—appears to decelerate and finally come to a halt.

C. Stable KK and KA complexes at $\epsilon < 0$

We have also considered the relevant coherent structure complexes in the case of $\epsilon \leq 0$. Similar to the situation at $\epsilon > 0$, complexes of both KK and KA types exist at $\beta < \beta_c$. Their existence limits are also shown in Fig. 4, whereas Fig. 7 showcases the dependence of the stability eigenvalues on β for given $\epsilon < 0$ and $\alpha = 0$. It can be seen here that the relevant imaginary eigenvalues approach 0 as β approaches β_c . A drastic difference from the case of $\epsilon > 0$ is that the KK complexes are *spectrally stable* whenever they exist at $\epsilon \leq 0$, once again in the full agreement with the analytical result for $\alpha = 0$, given by Eq. (31). The KA modes are *stable* too if the condition $\epsilon \leq 0$ is supplemented by $\alpha \leq \alpha_c$, for some appropriate finite critical value of the

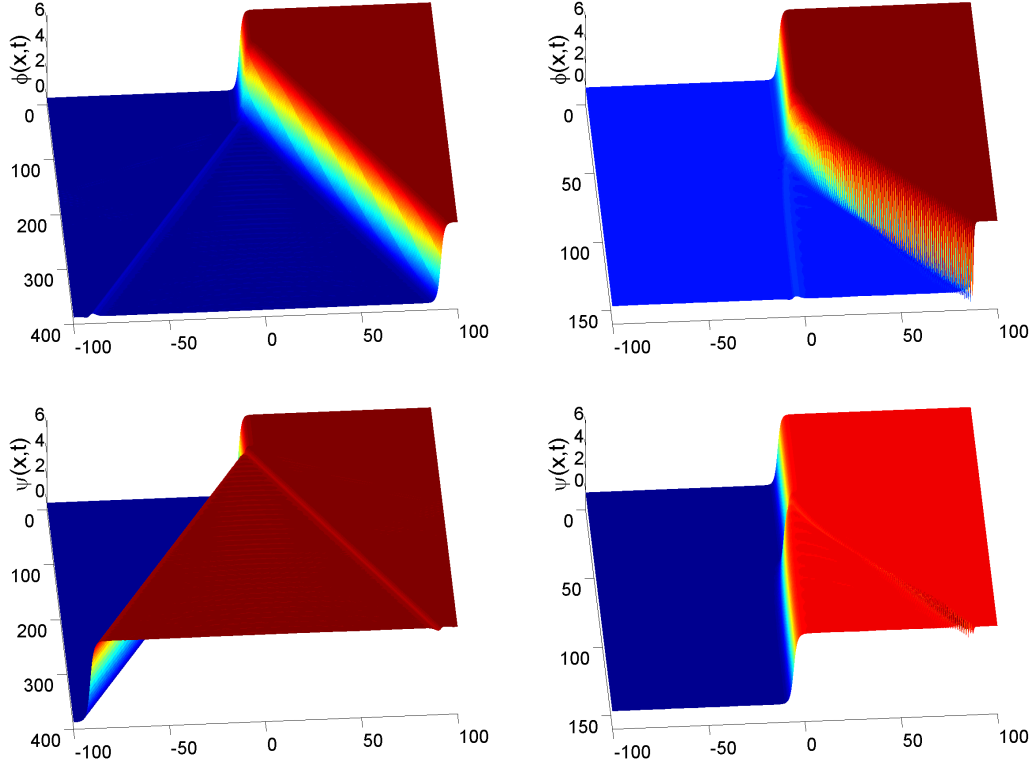


FIG. 5: (Color online) The evolution of unstable KK complexes. The top and bottom panels display components $\phi(x, t)$ and $\psi(x, t)$, respectively. In both cases, $\epsilon = 0.25$ and $\beta = 0.1$. In the left panels, $\alpha = 0$, and $\alpha = 0.05$ on the right-hand side.

gain-loss coefficient, $\alpha_c \leq \beta$ [i.e., α_c satisfies condition (14)]. Exactly at $\epsilon = 0$, the KK and KA only exist for $\beta = 0$ (notice that this is the uncoupled limit where ϕ and ψ are independent) and they are stable only for $\alpha = 0$ as, if $\alpha \neq 0$ for $\beta = 0$ the complexes are not stable because conditions (14)-(15) are violated. In this context, it is perhaps more precise to say that one component will be subject to damping, while the other subject to pumping, with the latter featuring unstable dynamics.

The KA solutions become exponentially unstable at $\alpha > \alpha_c$, as shown in Figs. 8 and 9. The latter figure shows that the instability splits the KA complex into two components. Naturally, the kink in the component (ψ) which is subject to the action of the dissipation comes to a halt, while its counterpart in the amplified component (ϕ) becomes a traveling one, accelerating over time. Each of the separated kink structures creates its “shadow” in the mate component, in the form of a dip.

The dependence of α_c on β is presented in Fig. 10. A noteworthy feature of this dependence is its non-monotonous form, with a maximum of α_c attained at a particular value of β , which depends on ϵ . This maximum is caused by the fact that, on the one hand, if β falls below a critical value, then $\alpha_c > \beta$ and condition (14) does not hold, hence the background (flat-state’s) instability masks the exponential instability; on the other hand, if β is above that critical value, then $\beta > \alpha_c$ and the latter instability manifests itself.

From a technical standpoint, it is relevant to note in passing that the finite difference discretization of the first order spatial and temporal derivatives introduces a number of additional, yet spurious numerical instabilities (associated with complex eigenvalues stemming from the continuous spectrum), disappearing as one approaches the continuum, infinite domain limit; see [25] for similar examples with temporal first derivatives in \mathcal{PT} -symmetric sine-Gordon and related systems, and [47] for such examples with spatial first derivatives in problems featuring Dirac operators. In what we have discussed above, we have not considered these instabilities, focusing on the true dynamical features of the continuum problem.

V. CONCLUSIONS AND FUTURE WORK

We have introduced a system of coupled sine-Gordon equations, with mutually balanced gain and loss in them, which represents the \mathcal{PT} symmetry in the system. Two types of coupling were included: sinusoidal terms, and the cross-derivative coupling. The former coupling corresponds to a commonly utilized interaction term between the corresponding FK (Frenkel-

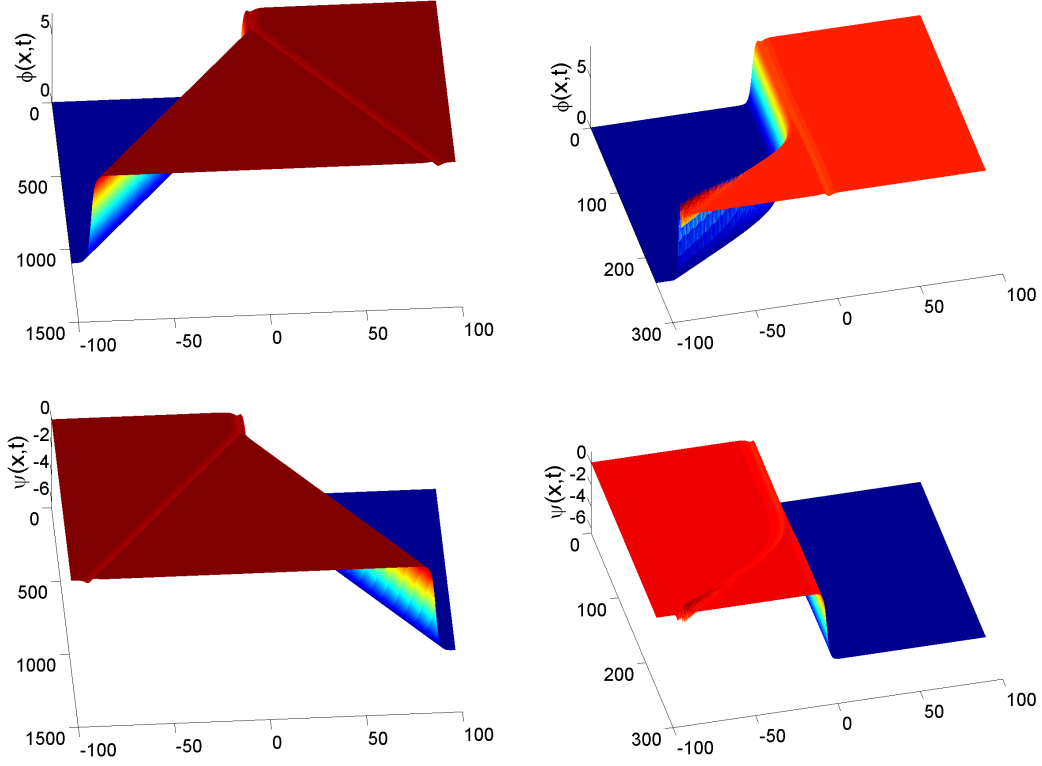


FIG. 6: (Color online) The evolution of unstable KA complexes. The panels have the same meaning as in Fig. 5, with the same values of ϵ , β , and α .

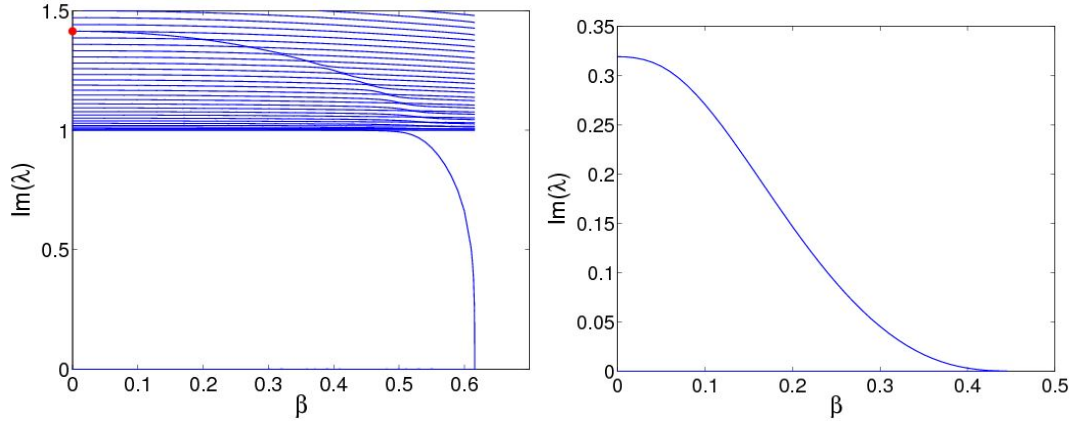


FIG. 7: (Color online) The dependence of the imaginary part of the stability eigenvalues on β at $\alpha = 0$ and $\epsilon = -1$ for *stable* KK and KA complexes (left and right panels, respectively). They exist up to the points at which $\text{Im}(\lambda)$ vanishes. The red dot at the left panel shows the exact prediction for the zero mode of (31)

Kontorova) chains. The cross-derivative coupling was not considered in previously studied models. It is proposed to be generated by three-body interactions, assuming that the particles belonging to parallel chains move along different directions. The KK (kink-antikink) and KA (kink-antikink) complexes were constructed in the system, and their stability was studied, by means of analytical and numerical methods. It has been found that the complexes are stable or unstable, depending on the sign of the sinusoidal coupling term. Stability regions for the complexes of both types were identified in the parameter space of the temporal gain/loss and the cross-derivative coupling strength. Simulations reveal splitting of unstable complexes into separating kinks and antikinks. The latter move at constant speed in the absence of gain and loss, and follow the dynamics imposed by the

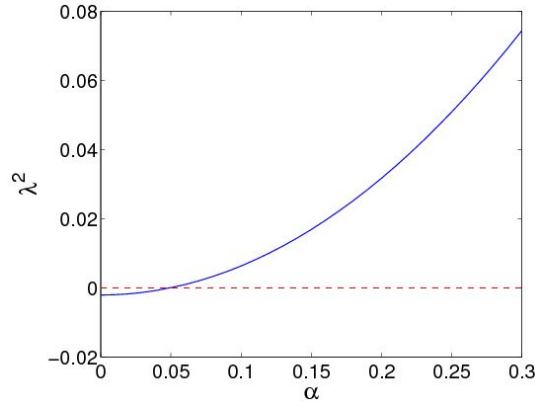


FIG. 8: (Color online) Squared instability eigenvalue for the KA complexes, versus the gain-loss coefficient, α , at $\beta = 0.3$ and $\epsilon = -1$.

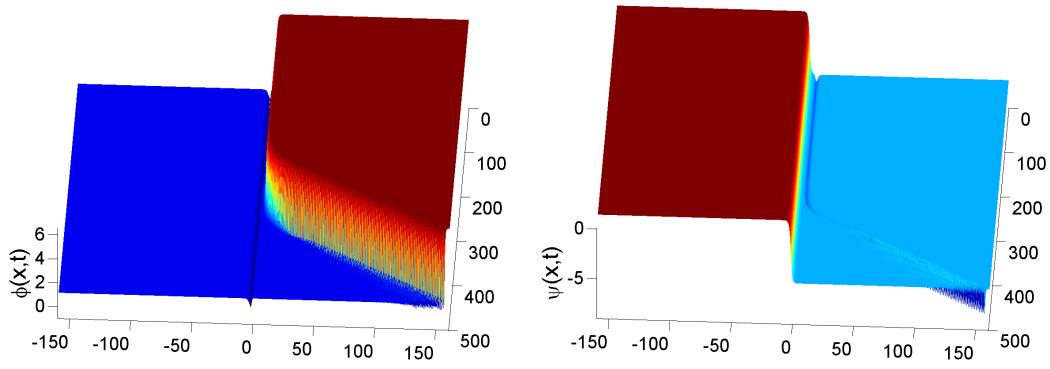


FIG. 9: (Color online) The evolution of an unstable KA solution at $\epsilon = -1$, $\beta = 0.3$ and $\alpha = 0.08$. To amplify effects of the true exponential instability, against the spurious instability of the background (see the text), the onset of the instability was catalyzed by adding an initial perturbation proportional to the corresponding eigenmode.

gain (acceleration) or loss (deceleration) in their presence.

There remain numerous interesting issues to address as a continuation of the present work. In particular, the possibility of the existing of stable traveling KK and KA complexes is a challenging problem. Moreover, a potentially analytical or semi-analytical study in the spirit of [48] could provide a set of guidelines on the expected motion (and stability) of the kinks in the presence of the additional terms considered herein. It is interesting too to identify stability boundaries for \mathcal{PT} -symmetric solitons of the NLS type in the framework of Eqs. (17) and (18) with $\beta \neq 0$. Finally, while we have explored the existence of kink-like stationary complexes, an exploration based on the NLS reduction of breather type solutions of different amplitudes (and of their amplitude and center of mass evolution) would also be of interest. A number of these topics are presently under consideration and will be reported in future studies.

-
- [1] B. A. Malomed and H. G. Winful, Phys. Rev. E **53**, 5365 (1996); J. Atai and B. A. Malomed, *ibid.* **54**, 4371 (1996).
 - [2] B. A. Malomed, Chaos **17**, 037117 (2007).
 - [3] A. Marini, D. V. Skryabin, and B. A. Malomed, Opt. Exp. **19**, 6616 (2011); C. Milián, D. E. Ceballos-Herrera, D. V. Skryabin, and A. Ferrando, Opt. Lett. **37**, 4221 (2012); Y. Xue, F. Ye, D. Mihalache, N. C. Panoiu, and X. Chen, Laser Phot. Rev. **8**, L52 (2014).
 - [4] P. V. Paulau, D. Gomila, P. Colet, N. A. Loiko, N. N. Rosanov, T. Ackemann, and W. J. Firth, Opt. Exp. **18**, 8859 (2010); P. V. Paulau, D. Gomila, P. Colet, B. A. Malomed, and W. J. Firth, Phys. Rev. E **84**, 036213 (2011).
 - [5] N. Akhmediev and A. Ankiewicz, *Dissipative Solitons* (Springer: Berlin, 2005).
 - [6] J. Atai and B. A. Malomed, Phys. Lett. A **246**, 412 (1998).
 - [7] B. A. Malomed, Physica D **29**, 155 (1987); S. Fauve and O. Thual, Phys. Rev. Lett. **64**, 282 (1990); I. V. Barashenkov, N. V. Alexeeva, and E. V. Zemlyanaya, *ibid.* **89**, 104101 (2002).

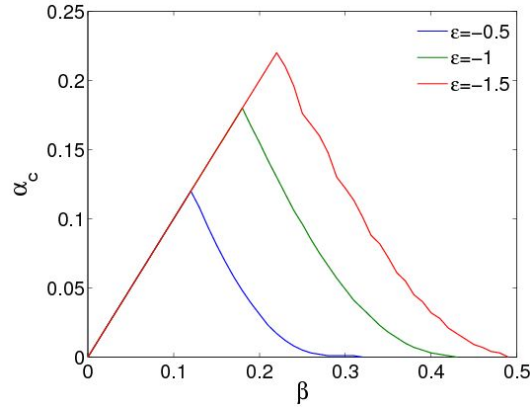


FIG. 10: (Color online) The critical value of the gain-loss coefficient, α_c , above which the KA complexes are unstable at $\epsilon < 0$, versus β .

- [8] A. Hasegawa and Y. Kodama, *Solitons in optical communications* (Clarendon Press, Oxford, 1995); Y. S. Kivshar and G. P. Agrawal, *Optical Solitons: From Fibers to Photonic Crystals* (Academic Press, San Diego, 2003).
- [9] C. M. Bender and S. Boettcher, Phys. Rev. Lett. **80**, 5243 (1998); C. M. Bender, D. C. Brody, and H. F. Jones, *ibid.* **89**, 270401 (2002); C. M. Bender, Rep. Prog. Phys. **70**, 947 (2007).
- [10] S. Longhi, Appl. Phys. B **104**, 453 (2011).
- [11] A. Ruschhaupt, F. Delgado and J. G. Muga, J. Phys. A: Math. Gen. **38**, L171 (2005); R. El-Ganainy, K. G. Makris, D. N. Christodoulides, and Z. H. Musslimani, Opt. Lett. **32**, 2632 (2007); M. V. Berry, J. Phys. A: Math. Theor. **41**, 244007 (2008); S. Klaiman, U. Günther, and N. Moiseyev, Phys. Rev. Lett. **101**, 080402 (2008); S. Longhi, Phys. Rev. Lett. **103**, 123601 (2009); S. Longhi, Phys. Rev. A **82**, 031801(R) (2010); K. Li and P. G. Kevrekidis Phys. Rev. E **83**, 066608 (2011); H. Ramezani, D. N. Christodoulides, V. Kovanis, I. Vitebskiy, and T. Kottos, Phys. Rev. Lett. **109**, 033902 (2012); M.-A. Miri, A. Regensburger, U. Peschel, and D. N. Christodoulides, Phys. Rev. A **86**, 023807 (2012).
- [12] A. Guo, G. J. Salamo, D. Duchesne, R. Morandotti, M. Volatier-Ravat, V. Aimez, G. A. Siviloglou, and D. N. Christodoulides, Phys. Rev. Lett. **103**, 093902 (2009); C. E. Rüter, K. G. Makris, R. El-Ganainy, D. N. Christodoulides, M. Segev, and D. Kip, Nature Phys. **6**, 192 (2010); A. Regensburger, C. Bersch, M.-A. Miri, G. Onishchukov, D. N. Christodoulides, and U. Peschel, Nature **488**, 167 (2012); M. Wimmer, A. Regensburger, M.-A. Miri, C. Bersch, D.N. Christodoulides and U. Peschel, Nature Communications **6**, 7782 (2015).
- [13] K. G. Makris, R. El-Ganainy, D. N. Christodoulides, and Z. H. Musslimani, Int. J. Theor. Phys. **50**, 1019 (2011).
- [14] S.V. Suchkov, A.A. Sukhorukov, J. Huang, S.V. Dmitriev, C. Lee, Yu, S. Kivshar, arXiv:1509.03378.
- [15] Z. H. Musslimani, K. G. Makris, R. El-Ganainy, and D. N. Christodoulides, Phys. Rev. Lett. **100**, 030402 (2008); F. Kh. Abdullaev, Y. V. Kartashov, V. V. Konotop, and D. A. Zezyulin, Phys. Rev. A **83**, 041805(R) (2011); Z. Shi, X. Jiang, X. Zhu, and H. Li, *ibid.* **84**, 053855 (2011); X. Zhu, H. Wang, L.-X. Zheng, H. Li, and Y.-J. He, Opt. Lett. **36**, 2680 (2011); J. Zeng and Y. Lan, Phys. Rev. E **85**, 047601 (2012); M.-A. Miri, A. B. Aceves, T. Kottos, V. Kovanis, and D. N. Christodoulides, Phys. Rev. A **86**, 033801 (2012); Y. He, X. Zhu, D. Mihalache, J. Liu, and Z. Chen, Opt. Commun. **285**, 3320 (2012); C. Li, H. Liu, and L. Dong, Opt. Exp. **20**, 16823 (2012); A. Khare, S. M. Al-Marzoug, and H. Bahloul, Phys. Lett. A **376**, 2880 (2012).
- [16] D. A. Zezyulin, Y. V. Kartashov, and V. V. Konotop, EPL **96**, 64003 (2011); S. Nixon, L. Ge, and J. Yang, Phys. Rev. A **85**, 023822 (2012).
- [17] H. Cartarius and G. Wunner, Phys. Rev. A **86**, 013612 (2012).
- [18] J.-Y. Lien, Y.-N. Chen, N. Ishida, H.-B. Chen, C.-C. Hwang, and F. Nori, Phys. Rev. B **91**, 024511 (2015).
- [19] R. Driben and B. A. Malomed, Opt. Lett. **36**, 4323 (2011); EPL **96**, 51001 (2011); N. V. Alexeeva, I. V. Barashenkov, A. A. Sukhorukov, and Y. S. Kivshar, Phys. Rev. A **85**, 063837 (2012); I. V. Barashenkov, S. V. Suchkov, A. A. Sukhorukov, S. V. Dmitriev, and Y. S. Kivshar, *ibid.* **86**, 053809 (2012).
- [20] I. V. Barashenkov, G. S. Jackson, and S. Flach, Phys. Rev. A **88**, 053817 (2013); S. V. Suchkov, S. V. Dmitriev, A. A. Sukhorukov, I. V. Barashenkov, E. R. Andriyanova, K. M. Dadgetdinova, and Y. S. Kivshar, Appl. Phys. A: Mat. Sci. Processing **115**, 443 (2014).
- [21] R. Driben and B. A. Malomed, EPL **99**, 54001 (2012).
- [22] P. Li, L. Li and B. A. Malomed, Phys. Rev. E **89**, 062926 (2014).
- [23] J. Čtyroký, V. Kuzmiak, and S. Eyderman, Opt. Exp. **18**, 21585 (2010); N. V. Alexeeva, I. V. Barashenkov, K. Ruyanov, and S. Flach, Phys. Rev. A **89**, 013848 (2014); S. Savoia, G. Castaldi, V. Galdi, A. Alú, and N. Engheta, Phys. Rev. B **89**, 085105 (2014); B. Dana, A. Bahabad, and B. A. Malomed, Phys. Rev. A **91**, 043808 (2015).
- [24] F. C. Moreira, V. V. Konotop, and B. A. Malomed, Phys. Rev. A **87**, 013832 (2013); K. Li, D. A. Zezyulin, P. G. Kevrekidis, V. V. Konotop, and F. Kh. Abdullaev, *ibid.* **88**, 053820 (2013); D. A. Antonosyan, A. S. Solntsev, and A. A. Sukhorukov, Opt. Lett. **40**, 4575 (2015).
- [25] A. Demirkaya, D.J. Frantzeskakis, P.G. Kevrekidis, A. Saxena and A. Stefanov, Phys. Rev. E **88**, 023203 (2013); A. Demirkaya, T. Kapitula, P.G. Kevrekidis, M. Stanislavova, A. Stefanov, Stud. Appl. Math. **133**, 298 (2014); N. Lu, P. G. Kevrekidis, and J. Cuevas-Maraver, J. Phys. A: Math. Theor. **47**, 455101 (2014).
- [26] A. Scott, Riv. Nuovo Cim. **27**, 1 (2004); J. Cuevas-Maraver, P. G. Kevrekidis, and F. Williams, editors: *The sine-Gordon Model and its Applications: From Pendula and Josephson Junctions to Gravity and High-Energy Physics* (Springer: Heidelberg, 2014).
- [27] O. M. Braun, Yu. S. Kivshar, and A. M. Kosevich, J. Phys. C **21**, 3881 (1988).
- [28] O. M. Braun and Y. S. Kivshar, *The Frenkel-Kontorova Model: Concepts, Methods, and Applications* (Springer-Verlag: Berlin 2004).

- [29] B. D. Josephson, Phys. Lett. **1**, 251 (1962); D. W. McLaughlin and A. C. Scott, Phys. Rev. A **18**, 1652 (1978); A. Barone and G. Paternó, *Physics and Applications of the Josephson Effect* (John Wiley & Sons: New York 1982); A. V. Ustinov, Physica D **123**, 315 (1998).
- [30] G. L. Lamb, Jr., Rev. Mod. Phys. **43**, 99 (1971).
- [31] V. G. Bar'yakhtar, B. A. Ivanov, M. V. Chetkin, Usp. Fiz. Nauk **146**, 417 (1985) [Sov. Phys. Uspekhi **28**, 564 (1985)].
- [32] J. Pouget and G. A. Maugin, Physica D **14**, 88 (1984).
- [33] S. Coleman, Phys. Rev. D **11**, 2088 (1975); L. D. Faddeev and V. E. Korepin, Phys. Rep. **42**, 1 (1978); R. Rajaraman, *Solitons and Instantons* (North Holland: Amsterdam 1982); A. O. Gogolin, A. A. Nersesyan, and A. M. Tsvelik, *Bosonization and Strongly Correlated Systems* (Cambridge University Press: Cambridge 2004).
- [34] Y. S. Kivshar and B. A. Malomed, Rev. Mod. Phys. **61**, 763 (1989).
- [35] M. V. Mineev, G. S. Mkrtchyan, and V. V. Schmidt, J. Low Temp. Phys. **45**, 497 (1981); A. F. Volkov, Pis'ma Zhurn. Eksp. Teor. Fiz. **45**, 299 [JETP Lett. **45**, 376 (1987)]; Y. S. Kivshar and B. A. Malomed, Phys. Rev. B **37**, 9325 (1988).
- [36] A. V. Ustinov, H. Kohlstedt, M. Cirillo, N. F. Pedersen, G. Hallimanns, and G. Heident, Phys. Rev. B **48**, 10614 (1993); S. Sakai, A. V. Ustinov, H. Kohlstedt, A. Petraglia, and N. F. Pedersen, *ibid.* **50**, 12905 (1994).
- [37] S. Savel'ev, V. A. Yampol'skii, A. L. Rakhmanov, and F. Nori, Rep. Progr. Phys. **73**, 026501 (2010).
- [38] S. P. Yukon and B. A. Malomed, J. Math. Phys. **56**, 091509 (2015).
- [39] R. Kleiner and P. Müller, Phys. Rev. B **49**, 1327 (1994).
- [40] S. Takeno and S. Homma, J. Phys. Soc. Jpn. **55**, 65 (1986); J. Phys. Soc. Jpn. **55**, 2547 (1986); J. Phys. Soc. Jpn. **56**, 3480 (1986); J. Phys. Soc. Jpn. **60**, 1931 (1991).
- [41] S. Takeno and S. Homma, Prog. Theor. Phys. **70**, 308 (1983).
- [42] O. M. Braun, T. P. Valkering, J. H. J. van Opheusden, and H. J. W. Zandvliet, Surface Science **384**, 129 (1997); A. Bylinskii, D. Gangloff, and V. Vuletić, Science **348**, 1115 (2015).
- [43] H. Yan, X. Li, B. Chandra, G. Tulevski, Y. Wu, M. Freitag, W. Zhu, P. Avouris, and F. Xia, Nature Nanotechnology **7**, 330 (2012).
- [44] E. J. R. Vesseur, T. Coenen, H. Caglayan, N. Engheta, and A. Polman, Phys. Rev. Lett. **110**, 013902 (2013).
- [45] K. S. Chiang, Opt. Lett. **20**, 997 (1995); K. S. Chiang, J. Opt. Soc. Am. B **14**, 1437 (1997).
- [46] R. Bullough, P. Caudrey, and G. Gibbs, in *Solitons*, ed. by R. K. Bullough and P. J. Caudrey (Springer-Verlag: Berlin, 1980).
- [47] J. Cuevas-Maraver, P. G. Kevrekidis, and A. Saxena, J. Phys. A: Math. Theor. **48**, 055204 (2015).
- [48] P. G. Kevrekidis, Phys. Rev. A **89**, 010102(R) (2014).